

Effects of quaternary alloying additions on the behaviour of Cu-8%Al-9%Mn alloy

Ali Hubi Haleem^a, Haydar H.J. Jamal Al-Deen^b, Doaa Amer Ali^c

a,b Department of Metallurgical Engineering, Materials Engineering Faculty, University of Babylon, Iraq.

c Materials Engineering, University of Babylon, Iraq.

Abstract. Corrosion is described as a common problem across many industries. In this study, the effect of Indium (In) and Tantalum (Ta) elements addition on behavior of Cu8Al9Mn shape memory alloys was investigated. Ta and In additions were made by (1,2 and 3)% wt.. Seven alloys were produced by powder metallurgy method (Cu-8Al-9Mn, Cu-8Al-9Mn-1%Ta, Cu-8Al-9Mn-2%Ta, Cu-8Al-9Mn-3%Ta, Cu-8Al-9Mn-1%In, Cu-8Al-9Mn-2%In and Cu-8Al-9Mn-3%In). A solution heating remediation at 900°C for 30 min. and then aging at 300°C for 1 hr. the remediation was performed after sintering at 950 °C for 4 hr. The effect of (Ta and In) alloys additives was investigated by utilizing X-rays diffraction (XRD), Vickers microhardness, deferential scanning calorimetry (DSC). For erosion test, a device designed & built based on ASTM G73 standard in corrosive media of 3.5% NaCl. The results demonstrated that an increase in hardness with the addition of elements and an improvement in the resistance of the alloy to erosion corrosion due to the (formation of the intermetallic compounds, as well as an increase in the hardness and creation of oxide layer which have great cohesion with alloy surface). XRD analysis demonstrated that the kind of martensitic form is 18R (β_1 Cu₃Al) and little amount of γ martensite with thick plate shape. Alloys with added (Ta) element demonstrated better improvement in erosion corrosion resistance up to 85.30% at 3%Ta compared to 66.70 % at 3% In. **Keywords:** Powder metallurgy, CuAlMn alloys, Erosion corrosion, Indium addition, Tantalum addition.

Introduction

Super elasticity (SE) and shape memory effect (SME) are good phenomena, which demonstrate in Cu-Al-Mn alloys, and they make material appropriate to several application [1] such as components of smart actuators, sensors and dampers [2]. System CuAlMn SMAs are economical feasible and have great strength and excellent damping limit within their austenitic to martensitic phase transformation as compared with other systems as NiTi. Additionally, grain refining alloys elements to SMAs can influence Transformation temps (increase or decrease), shape effects and enhance stress cracking resistance produced during quenching [3]. In SMAs Cu-Al-Mn the β phase were disordered and stable at great temps and transforms to martensite on fast cooling from the austenitizing temps. The alloys leave meanwhile a succession of ordering reactions alter to martensite on fast cooling from the austenite temp $L_{21} \leftrightarrow B_2$ and $B_2 \leftrightarrow A_2$ [4]. The phases that can take place at greater and lower temps near to Cu₃Al composition could be determined as per following steps; 1) The disordered β phase (A_2 or body center cubic structure) is the balanced structure at elevated temps, 2) the balanced phases at low temps are α -Cu, T_3 -Cu₃Mn₂Al, γ_2 -Cu₉Al₄ and β -Mn phase[5-10]

Limiting flow velocity is one of the central problems to utilize of Cu base alloys with seawater for which these can be utilize without presence of erosion corrosion. It is important, however, to recognize that, in wear, material is removed from surfaces. The form of that removal can take place in various manners according to the mechanisms operating in the system. The creation and growth of the Copper oxide layer in Cu base alloy in sea-water accompany with a reduction in the rate of ionic migration in the oxide films should lead to a good resistance to erosion-corrosion [11]. The erosion-corrosion describes as a relative movement of the corrosive fluid while the metallic material immersed in it. It is also can only be obtained by a mechanical movement, i.e pure mechanical erosion the solid particles scratch internal surface of wall leading to plastic deformation which makes the structure more active. Erosion corrosion might resulted in various forms such as grooves, waves, gullies, holes, and valleys [12,13]. Many factors can affect erosion corrosion such as velocity, turbulence, impingement, the presence of suspended solids, and temp[14,15,16].

In this work, Tantalum and Indium particles was added to Cu8Al9Mn shape memory alloys utilizing powder technology for enhancing performance of Cu8Al9Mn erosion corrosion resistance. The objective of the research is to investigate changes in microstructures, hardness, thermomechanical behaviour and erosion-corrosions performance in 3.5% wt NaCl (sea-water) solutions.

Experimental section

The purity of the utilized powders measured by utilizing X-ray fluorescent (XRF) and the particle size analysis was done by utilizing laser particle size analyzer kind "Bettersize" are demonstrated in Table 1.

Table 1. Averages particle size and purity of uses powders.

Powders	Average particle size (µm)	Purity%	Supplier
Copper	4.827	99.57	India/CDHchemical/Central Drug House (P) Ltd.
Aluminum	19.09	99.06	=
manganese	19.38	99.84	=
Tantalum	11.74	99.86	=
Indium	18.46	99.2	=

(A)Preparation of Specimens

The SMAs Cu8%Al9%Mn-X(Ta and In) were produce by PM method under an inert atmosphere (Argon), as demonstrated in Table 2, all specimens of Cu-Al-Mn alloys plus additives in weight percentage.

Table 2. Chemical Composition of alloys under study

Synthesized Composition	Analyzed Composition				
	Cu (%)	Al (%)	Mn (%)	Ta (%)	In (%)
Cu-8Al-9Mn	Bal	7.8	8.4	-	-
Cu-8Al-9Mn-1Ta	Bal	7.2	8.1	0.7	-
Cu-8Al-9Mn-2Ta	Bal	7.2	8.3	1.2	-
Cu-8Al-9Mn-3Ta	Bal	7.17	8.1	2.3	-
Cu-8Al-9Mn-1In	Bal	7.38	8	-	0.78
Cu-8Al-9Mn-2In	Bal	7.8	8.2	-	1.63
Cu-8Al-9Mn-3In	Bal	7	8.7	-	2.7

The quantity of Cu in the alloys changed depending on the weight of (Ta) and (In) components, whereas (Al) and (Mn) remained constant. In the first step, powders were combined for 4 hours in a planetary ball mill in the presence of ethanol (to prevent the friction between the powders particles and mold to decrease the powder particles oxidation throughout process of mixing). The combination has been cold compressed in the second step (compacting stage) utilizing an electric hydraulic press with compression pressure in a uni-axial direction (9.0 tons). As demonstrated in Fig. (1B) , cylindrical specimens with a diameter of 1.2 cm and a thickness of 0.5 cm were made.

The final step is sintering, that is a heating remediation that compacts green to create atom bonding. A quartz tube and two ends make up the sintering oven. In a quartz tube, an argon gas pump is utilized to create a vacuum environment (to avoid oxidation under great temps) at a rate of 2 bar/min. The sintering cycle's heating rate has been set at 10 degrees Celsius per minute. The next stage was incorporated in the specimen sintering process, as illustrated in (Fig. 1A).

- a. Heating from room temp to (550C°) and soaking for (2) hours
- b. Heating from (550C°) to (950C°) and soaking for (4) hours
- c. Slow cooling in the furnace with continues vacuum to room temp.

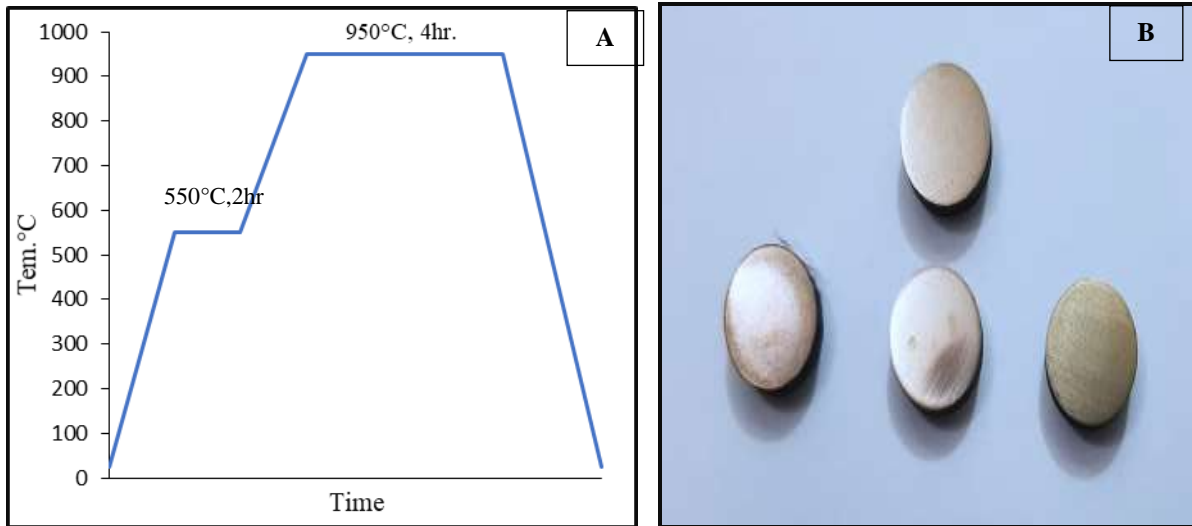


Fig. 1: A) sintering procedure, B) final products

(B) Thermo-mechanical heating remediation and tests

Heating remediation include two heating remediation (1) Solution heating remediation in which sinter specimen exposed to solution heating remediation as demonstrated in Fig. 2A. The purpose of step quenching was to reduce of creation quenching cracks and the restricts of marten site plates by excess dislocations trapped in fast cooling from great temp [17]. (2B) Ageing heating remediation after solution heating remediation the specimen (base alloys with and without additives) were exposed to post-quench isothermal ageing in the austenitic phase. Aging heating remediation cyclic demonstrate in Fig 2B.

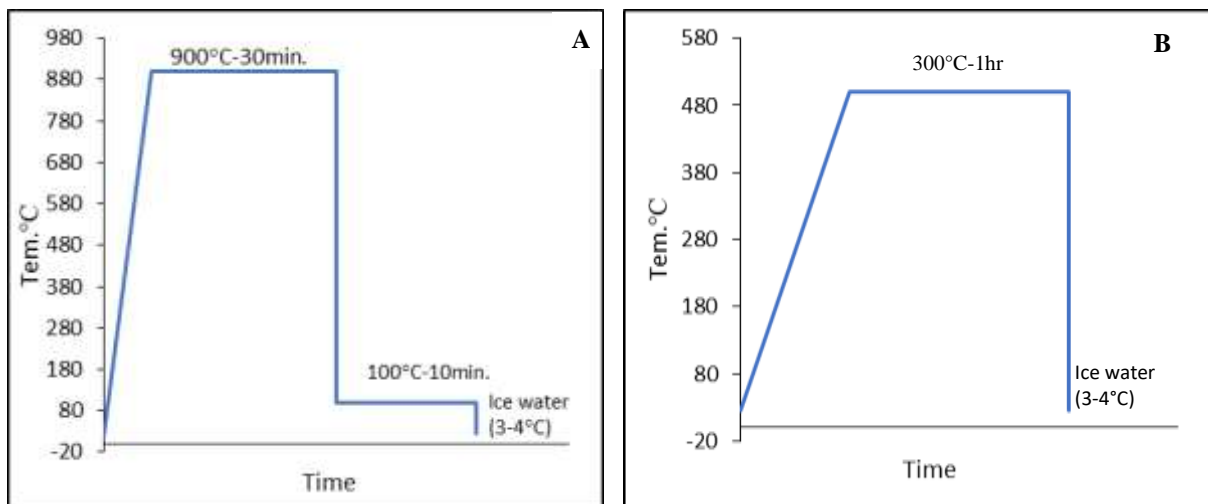


Fig. 2: (A) solution treatment, (B) aging treatment

The phases and crystal structures of the alloys were calculated utilizing X-ray diffraction device kind (shimadzu XRD-600 X-Ray diffractometer). XRD utilizing radiation $CuK\alpha$ with wave length ($\lambda=1,5409 \text{ \AA}$) 40 kV, 30 mA at $2\theta=20^\circ-80^\circ$. For optical microscope analysis Ageing specimens were ground by utilizing SiC paper grits as (180, 400, 800, 1000, 1200 and 2000) then polished by utilizing diamond solution (1 μ). The specimens were etched by “10 g $FeCl_3$ +25 ml HCL +100 ml distilled water” [16]. Microscopes kind 1280 XEQMM300TUSB was utilized. Vickers micro hardness devices kinds (Digital Micro Vickers Hardness Tester TH 717) utilizing a load of 500 g for 15 sec with a squares base diamonds pyramid. The erosion-corrosion instrument consists of motor (Q max 53 l/min, H max =38m, HP=1hp, 2850 rpm, Size 1in×1in), plastic tank, tubes to fall the water by nozzle on the specimen. All alloys examined at room temp (25°C), wherever salt solution (sea-water) will causing erosion-corrosion and fall from the nozzle at angle=90°. The nozzle is (2 mm) in diameter and fixed at distance of (10 mm) from the specimen. It is possible to calculate the change in weight and then get the erosion rate according to Eq. 1 as follow.

$$Erosion\ rate \left(\frac{mg}{hr} \right) = \frac{\Delta W}{time\ of\ exposure * time} \tag{1}$$

$\Delta W = \text{original weight (W}^\circ) - \text{weight after fixed time (W}_1, \text{W}_2, \dots)$

change in weight (Δw) = original weight (w°) - weight after fixed time ($w_1, 2, \dots$)

$$\text{Erosion rate } \left(\frac{\text{mg}}{\text{hr}} \right) = \frac{\Delta w}{\text{time of exposure}} \dots \dots \dots 2$$

Results and discussions

X-ray diffraction results (XRD)

Result of XRD paradigm of CAM SMAs with additives of (Ta and In) are presented in Fig. 3 and 4 after sintering and aging respectively. From Fig. (3 and 4) it was observed that the creation of phases which indicates the form of the both martensitic and austenite phase. The change in the intensity (I) of the diffraction of martensitic phases peaks based on the limit of austenite to martensite transformation. No variation has been detected in the kind of martensitic phase with additives, but the thickness of the martensite plate was decrease, as demonstrated in OM of the alloys. Results demonstrate the microstructures of alloys consist of β_1 and γ_1 martensites. In these graphs it is possible to verify the presence of Ta_2Al_3 when add Ta were determined [18,19].

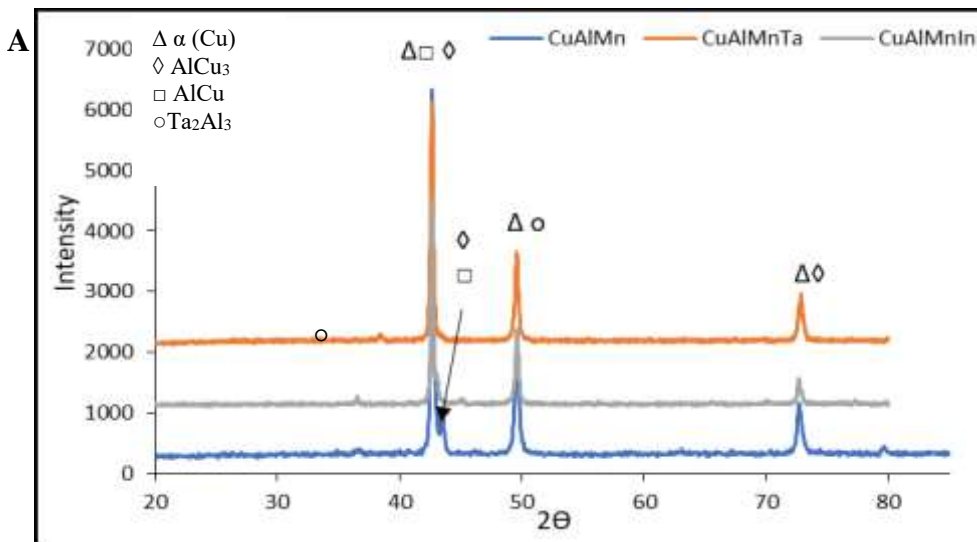


Fig. 3: XRD (A) after sintering

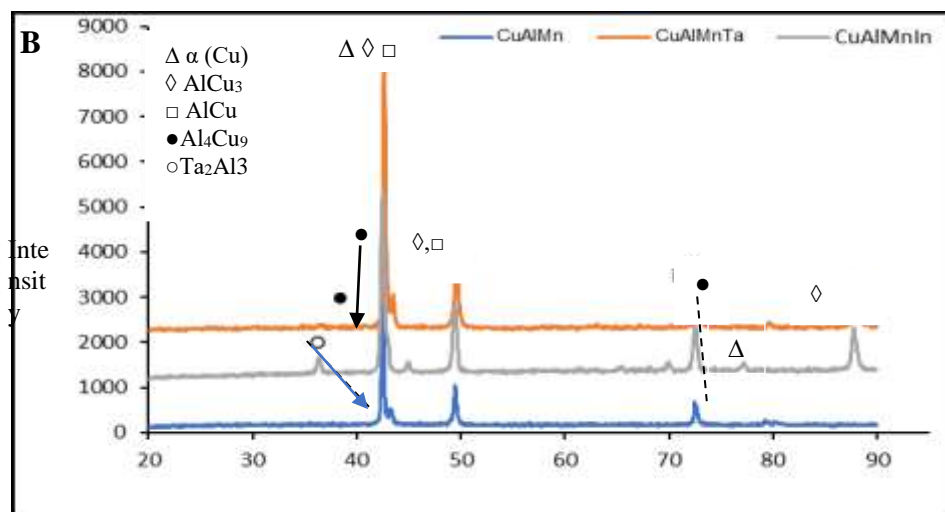


Fig. 4: XRD after quenching

Micro hardness result

Fig. 5. A in the aged specimen the hardness is 108.5 g./ μm^2 for base alloy (A) and increasing to (117, 120, 126.6 g./ μm^2) respectively with increase the Ta percentage addition. The best addition amount of Ta is 3 wt. % and this is attributed to the grains refinement which was associated with the inhibiting effects of grain growth by Ta element in solid solution. In the Figure (5.B) it was noticed that the addition of Indium with various amounts (1,2, and 3) % wt. affects the hardness of alloys in the aged condition, it increases to (111, 118, 132 g./ μm^2) with In addition. The Vickers hardness increased as the In content increased because of the combined effect of the solid-solution strengthening of the α -phase and the hardening of the fine martensitic phase [17, 18]

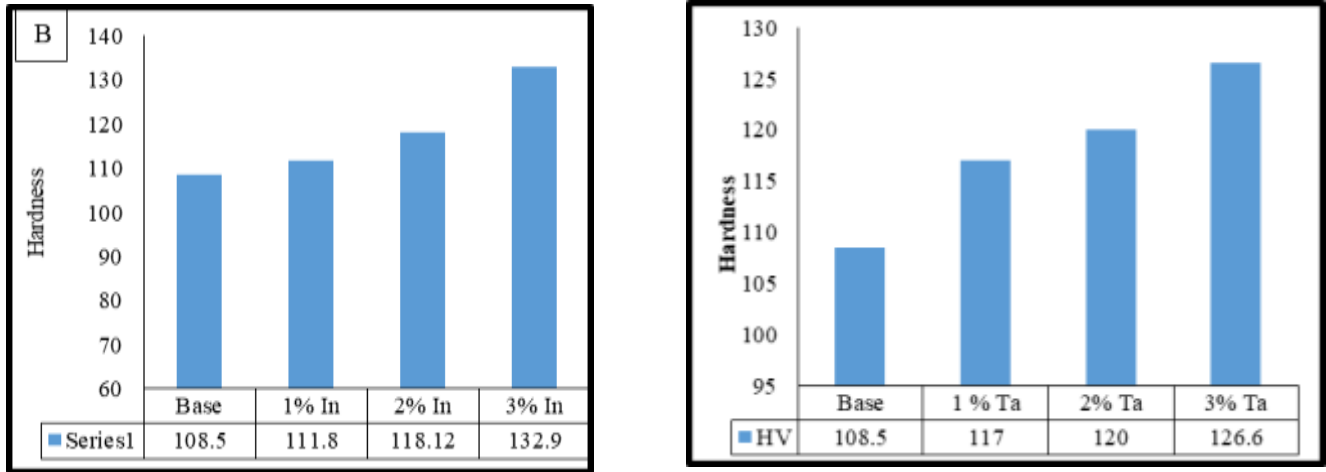


Fig. 5: Micro hardness measurements (A) CuAlMn-Ta and (B)CuAlMn-In

Erosion corrosion results

Fig. 6 and 7 explain the erosion corrosion behavior of base alloy without and with alloy additives (Ta and In) respectively in 3.5% NaCl Where the values were taken during the first hour for every quarter of an hour, then the second hour every half hour, and after that every hour, the specimen is washed with water and alcohol, then dried in hot air, and then the change the weight reading is taken. The increase in weight is due to several factors the first mechanical that occurs as a result of continuous movement and the second chemical that occurs as a result of the interaction of the corrosive medium with the specimen.

From the Fig. (6 and 7) we can notice that the alloys after adding elements (Tantalum and Indium) the corrosion rate is less as compared with the base alloy and the reason is that the hardness of the alloys increases with the addition of the three elements as demonstrated in the Fig. (6 and 7), and this increase enhance strengthens of alloys to resistance erosion, Increase the cohesion of the protective oxide layer by adding elements (Ta and In).The Table 3 represents the degradation wear rate and improvement rates for the alloys utilized.

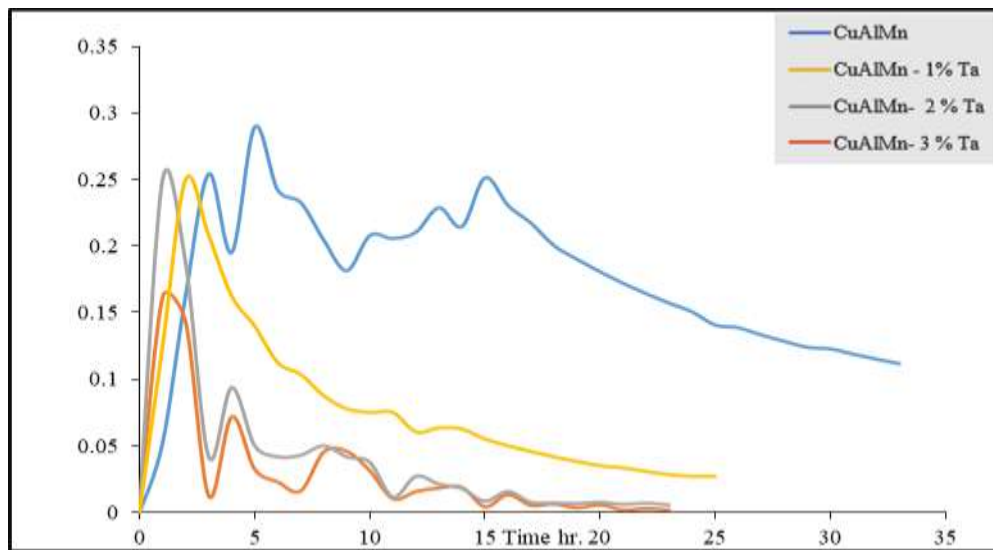


Fig. 6: Erosion corrosion rate for CuAlMn-x%Ta

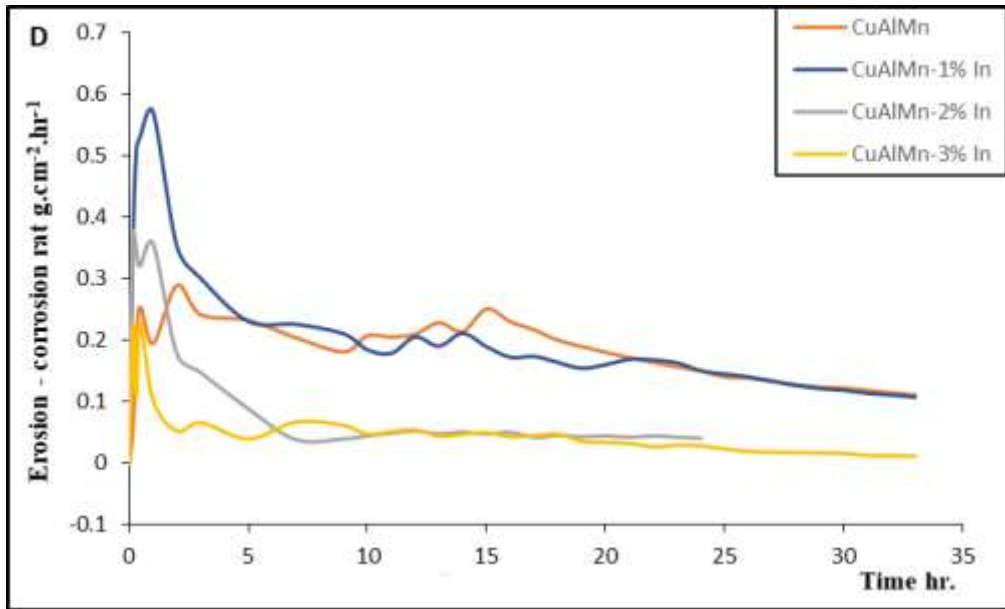


Fig. 7: Erosion corrosion rate for CuAlMn-x%In

Table 3: Erosion corrosion rate and enhancement for alloys

Synthesized Composition	Erosion rate	Improvement %
Cu-8Al-9Mn	0.122	0
Cu-8Al-9Mn-1%Ta	0.027	77.86885
Cu-8Al-9Mn-2%Ta	0.0017	98.60656
Cu-8Al-9Mn-3%Ta	0.0059	95.16393
Cu-8Al-9Mn-1%In	0.188
Cu-8Al-9Mn-2%In	0.044	63.93443
Cu-8Al-9Mn-3%In	0.0175	85.65574

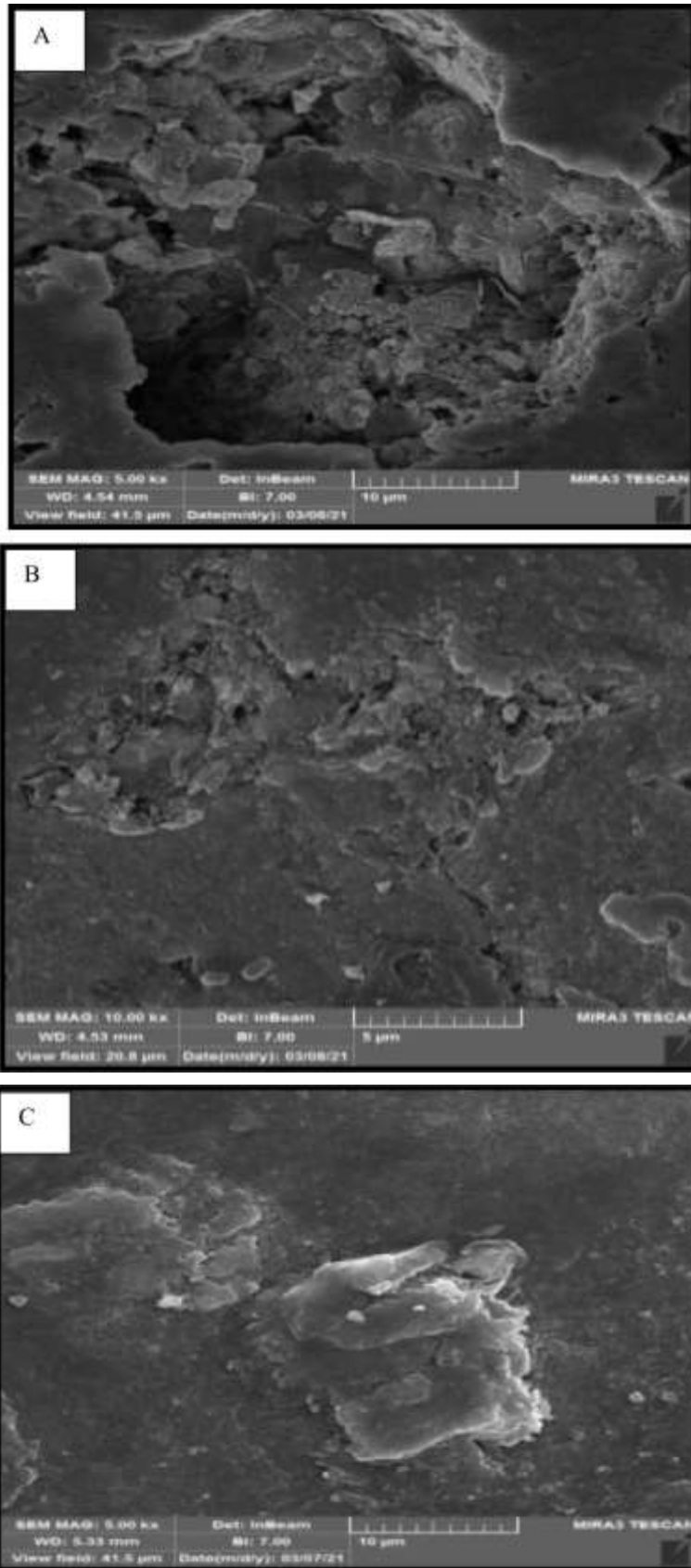


Figure (8): SEM analyses of surface morphology of (A)CuAlMn, (B) CuAlMn- 3% Ta, (C) CuAlMn- 3% In after erosion corrosion test with magnifications (5.00KX)

From Figures (8 – A, B, C) can be observed that the base alloy surface less resistance to erosion than the alloys with additive as the base alloy (CuAlMn) have less hardness (HV equal to 108.5) otherwise for CuAlMn-3%Ta, CuAlMn-3%In, the microhardness measurement reach to 126.6, 132.9 respectively.

Representative graphs of analysis for DSC analysis of Cu8Al9Mn, Cu8Al9Mn-3%Ta, Cu8Al9Mn-3%In SMA gained on heating from 0 °C until 600°C (5 °C min) on the as aging specimen demonstrated in Fig. 9. During heating, the reversal of phases has been refer to an abrupt change in resistive lope between 77°C and 277 °C. Such Thermal event has already been associated with the corresponds to the consumption of the $\beta_3(L_{21})$ -Cu₂MnAl phase for producing the $\beta_1(D0_3)$ -Cu₃Al phase . Therefore, the reaction can be represented by the $\beta_3(L_{21})$ -Cu₂MnAl + $\beta_1(D0_3)$ -Cu₃Al \rightarrow $\beta_1(D0_3)$ -Cu₃Al transformation. This transition is related to the Curie temp of alloys due to the ferromagnetic $\beta_3(L_{21})$ phase decomposition in which the D03 phase is dissolved in to the matrix [23, 24, 25]. The presence of peak at range 300°C in the curves may indicate that this disordering process occurs in two stages[26].

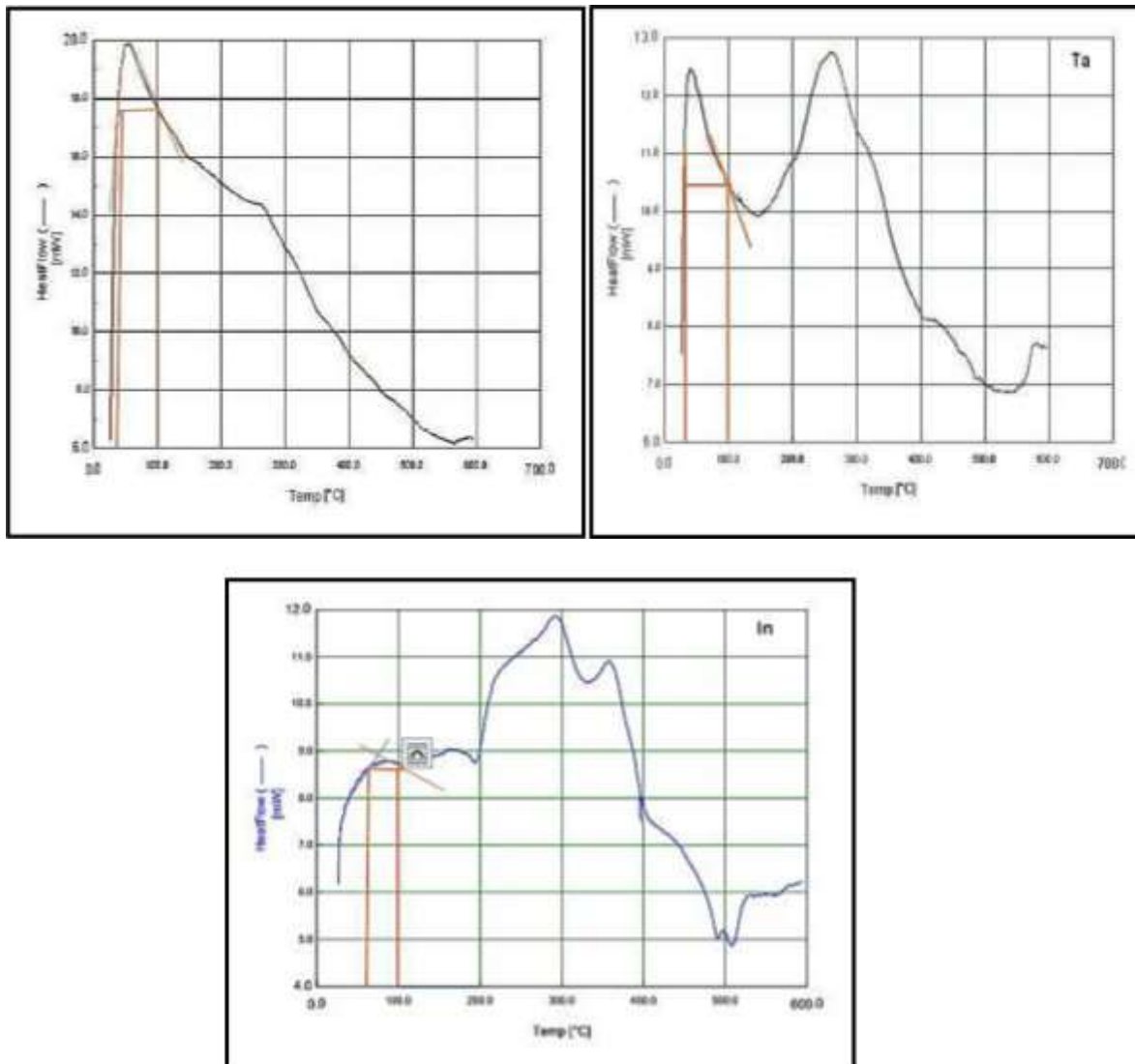


Fig. 9: DSC curves that were obtained at heating CuAlMn,CuAlMn-3% Ta, CuAlMn-3%In

Table 4: Transformation temps of CuAlMn alloys after aging in 300°C.

Synthesized Composition	Austanite start (As) in °C	Austanite finish(Af) in °C
Cu-8Al-9Mn	45	100
Cu-8Al-9Mn-3Ta	40	115
Cu-8Al-9Mn-3In	75	105

Optical microstructures (OM)

Optical microstructures of the Cu-Al-Mn specimens with quaternary addition is given in Fig. 10. At the betatization at 900 degree centigrade, the alloys have disordered β phase with a body center cubic structure. After solution heating remediation at 900 degree centigrade and quenching in ice water, the structure consist of β_1' martensite and β parent phase at room temp. The creation of

martensitic is observed in the specimens after quenched (austenite phase complete transformation to marten site phase). As observed in Fig. 9, all the specimens are formed from complete lath kind martensitic structure with thin martensitic plates or variations. The martensite variations with various orientations in each grain. These martensite variations are called as lath kinds a β_1' martensite with thick plates is detected in these alloys [23-24].

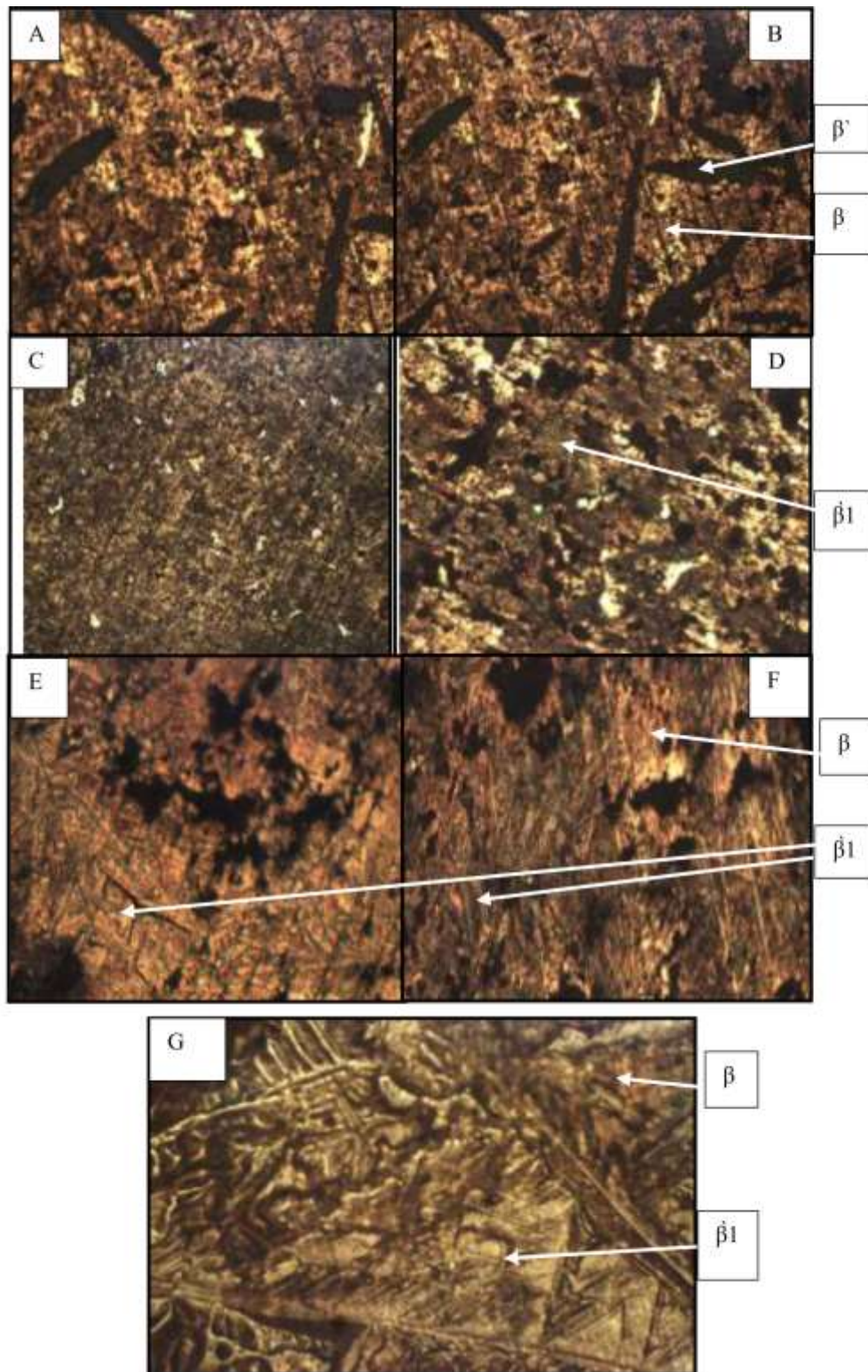


Fig. 10: OM of alloys A- CAM 1% Ta, B-CAM 2% Ta, C-CAM 3% Ta, D-CAM 1% In, E- CAM 2% In, F-CAM 3% In, G-CAM, CAM refer to CuAlMn

Conclusion

The alloy Cu8Al9Mn-X (Ta or In) was prepared utilizing a powder metallurgy method, then alloys elements (Tantalum and Indium) were added in three various proportions. From the XRD test it appears that three phases (α , β_1 and γ_1) are formed after aging heating remediation. By adding the element Tantalum with three percentage (1, 2 and 3) %wt. the hardness improved by (7, 10 and 16) %wt respectively, while by adding Indium (1, 2 and 3) %wt. the hardness was enhanced (3, 8 and 22)% respectively. From DSC test, detected small various in the temp peaks of the three alloys while heating. This fact suggest that the martensite transformations temp were not significantly affected by the alloy additives. The rate of metal loss in erosion is less with the addition of the elements (Ta and In) and that the element tantalum demonstrated greater resistance to erosion corrosion with increasing the percentage of addition and its stability is better compared to the base alloy.

References

- [1] R. O. Ferreira et.al , Thermal behavior of as-annealed CuAlMnAgZr alloys J. of Thermal Analysis and Calorimetry, (2020).
- [2] X. Chena et. al. ,Microstructure, superelasticity and shape memory effect by stress-induced martensite stabilization in Cu–Al–Mn–Ti shape memory alloys Materials Science & Engineering B **36-237**(2018) 10-17.
- [3] U. Arlica et. Al., Impact of Alloy Composition and Thermal Stabilization on Martensitic Phase Transformation Structures in CuAlMn Shape Memory Alloys Materials Research **21 2** (2018).
- [4] V. Sampath a1 and U. Mallik ,Influence of minor additions of boron and zirconium on shape memory properties and grain refinement of a Cu-Al-Mn shape memory alloy European Symposium on Martensitic Transformations EDP Sciences **05028** (2009).
- [5] C. Aksu et. al ,Thermal and structural alternations in CuAlMnNi shape memory alloy by the effect of various pressure applications Physica B **521** (2017)331–338.
- [6] T. Omori et. Al, Superplasticity of Cu-Al-MnNi shape memory alloy Mater. Trans. **11** (2007)2914–2918.
- [7] Y. Sutou et. al. ,Effects of ageing on bainitic and thermally induced martensitic transformations in ductile Cu-Al-Mn based shape memory alloys Acta Mater ,(2009) 5748–5758 .
- [8] Kainuma et. al. , Thermoelastic martensite and shape memory effect in ductile Cu-Al-Mn alloys Metal Mater. Trans. **27** (1996) 2187–2195.
- [9] C. Canbay and Z. Karagoz, The effect of quaternary element on the thermodynamic parameters and structure of CuAlMn shape memory alloys Appl. Phys, (2013).
- [10] De Sanchez et. al. ,The use of great speed rotating disc electrodes for the study of erosion-corrosion of copper base alloys in sea water Corrosion Science **28** (1988)141-151.
- [11] Lekan p. et. al. , Corrosion Problems during Oil and Gas Production and its Mitigation I. J. of Industrial Chemistry **41**(2013) 35.
- [12] Zaki A. ,Principles of corrosion engineering and corrosion control I. Chem. E. , No. First Edition USA, 2006.
- [13] Philip S. , Fundamentals of corrosion mechanism, causes and preventative methods United States of America: Taylor and Francis Group, 2006.
- [14] Roshan Kuruvila et. al. ,A brief review on the erosion-corrosion behaviour of engineering materials Corros Rev, 2018 .
- [15] S. Rajahram et. al. Erosion–corrosion resistance of engineering materials in various test conditions Wear 267 (2009) 244–254.
- [16] X. Chena et. al. ,Microstructure, superelasticity and shape memory effect by stress-induced martensite stabilization in Cu–Al–Mn–Ti shape memory alloys, Materials Science & Engineering B, **236–237** (2018) 10–17.
- [17] H. Alfay et. al. , Effect of Ta addition on hardness and wear resist of Cu-Al-Ni shape memory alloy fabricated by powder metallurgy 6560 (2018)141.
- [18] S. Saud, Effect of Ta Additions on the microstructure damping and shape memory behaviours of pre alloyed Cu-AlNi Shape Memory Alloys Hindawi **13** (2017).
- [19] C. Pilz et. al. ,Microstructure and phase stability of CuAlMnAgZr multicomponent alloys Materials Chemistry and Physics **241** (2020) 22343.
- [20] C. Santosa et. al., Effects of Ag presence on phases separation and order-disorder transitions in Cu-xAl-Mn alloys, Materials Chemistry and Physics **227** (2019) 184-190.
- [21] A. Adorno et. al. ,Thermal behaviour of CuAl alloy near the α -CuAl solubility limit J. of Thermal Analysis and Calorimetry **65** (2001) 221–229.
- [22] V. Pelosin and A. Riviere ,Structural and mechanical spectroscopy study of the b9 martensite 1 decomposition in Cu-12% Al-3% Ni(wt.%) alloy J. of Alloys and Compounds **268** (1998)166–172.
- [23] R. O. Ferreira , L. S. Silva , R. A. G. Silva, Thermal behavior of asannealed CuAlMnAgZr alloys, Journal of Thermal Analysis and Calorimetry (2020).
- [24] C.B. Pilz , E.L. Matsumura , A. Paganotti , D.R. Cornejo , R.A.G. Silva, Microstructure and phase stability of CuAlMnAgZr multicomponent alloys,Materials Chemistry and Physics,241 (2020)122343.
- [25] C. Santosa , A. Adornoa , M. Stipcichc, Cunibertic, , J. Souzaab , C. Bessab , R. Silvab, Effects of Ag presence on phases separation and orderdisorder transitions in Cu-xAl-Mn alloys, Materials Chemistry and Physics,227 ,(2019),184–190
- [26] .A. T. Adorno, M. R. Guerreiro and A. V. Benedetti, thermal behaviour of CuAl alloy near the α -CuAl solubility limit, Journal of Thermal Analysis and Calorimetry ,65 (2001) 221–229.